



18 **Abstract**

19 Mammalian hibernators survive prolonged periods of cold and resource scarcity by  
20 temporarily modulating normal physiological functions, but the mechanisms underlying these  
21 adaptations are poorly understood. The hibernation cycle of thirteen-lined ground squirrels lasts  
22 for 5–7 months and comprises weeks of hypometabolic, hypothermic torpor interspersed with  
23 24–48-hour periods of an active-like interbout arousal (IBA) state. We show that ground squirrels,  
24 who endure the entire hibernation season without food, have negligible hunger drive during  
25 IBAs. These squirrels exhibit reversible inhibition of the hypothalamic feeding center, such that  
26 hypothalamic arcuate nucleus neurons exhibit reduced sensitivity to the orexigenic and  
27 anorexigenic effects of ghrelin and leptin, respectively. However, hypothalamic infusion of  
28 thyroid hormone during an IBA is sufficient to rescue hibernation anorexia. Our results reveal  
29 that thyroid hormone deficiency underlies hibernation anorexia and demonstrate the functional  
30 flexibility of the hypothalamic feeding center.

31 Hibernation was first documented in 350 BCE by Aristotle, who noted that some creatures  
32 cease eating and conceal themselves in a sleep-like state for many months to pass the winter<sup>1</sup>.  
33 Hibernation invokes a series of flexible adaptations that allow animals to thrive in inhospitable  
34 environments, where they experience thermal challenges and food scarcity<sup>2</sup>. Coordination of  
35 hunger and satiety is essential for hibernators to survive, as premature emergence from  
36 underground burrows to seek food may dysregulate dependent processes and increase the risk  
37 of predation.

38 In thirteen-lined ground squirrels (*Ictidomys tridecemlineatus*), hibernation consists of repeated  
39 cycles of hypothermic torpor interspersed with brief periods of euthermic IBA (Fig. 1a, b). During  
40 torpor, animals enter a state of suspended animation by profoundly reducing their metabolic,  
41 heart and respiration rates, and lowering their body temperature to 2–4 °C. Every 2–3 weeks,  
42 squirrels arouse to spend ~24 hours in IBA, when their main bodily functions temporarily return  
43 to an active-like state (Fig. 1b)<sup>3</sup>. Ground squirrels do not depend on stored food for fuel during  
44 hibernation; instead, energy is supplied by body fat amassed during the summer. Thus, although  
45 hibernating squirrels resemble fasted animals metabolically, they demonstrate little interest in  
46 food despite enduring over seven months of starvation<sup>4–7</sup>. We sought to understand the  
47 mechanism underlying this remarkable example of reversible anorexia by comparing euthermic  
48 animals during the active season with euthermic animals during IBAs in the hibernation season.  
49 These experiments reveal that thyroid hormone deficiency in the hypothalamus underlies  
50 hibernation anorexia.

51

## 52 **Results**

### 53 **Hibernating ground squirrels have negligible hunger drive**

54 When squirrels were presented with food during the numerous IBAs throughout the hibernation  
55 season, they consumed approximately six times less food than during the active state (active:  
56  $14.0 \pm 0.8$  g/day; IBA:  $2.4 \pm 0.2$  g/day; Fig. 1c). Their body weight continuously decreased  
57 throughout hibernation, reaching ~50% of their starting weight by the end of the season (Fig. 1c).  
58 During IBAs, we found reduced levels of serum glucose (active:  $22.2 \pm 2.9$  mM; IBA:  $12.8 \pm 1.1$   
59 mM) and serum insulin (active:  $44.4 \pm 7.4$   $\mu$ U/mL; IBA:  $8.4 \pm 1.3$   $\mu$ U/mL), both of which decreased

60 throughout hibernation (Fig. 1d, e). Consistent with metabolism of fat being the primary energy  
61 source during hibernation, squirrels exhibited increased levels of serum  $\beta$ -hydroxybutyrate  
62 during IBAs compared to active squirrels (active:  $0.23 \pm 0.04$  mM; IBA:  $2.07 \pm 0.25$  mM; Fig. 1f).  
63 Thus, squirrels appear to lack hunger drive during hibernation, even during IBAs.

64

### 65 **Hibernating squirrels demonstrate reversible resistance to ghrelin**

66 During fasting, the stomach releases the orexigenic hormone ghrelin, which activates Agouti-  
67 Related Peptide/Neuropeptide Y (AgRP/NPY) neurons in the arcuate nucleus of the  
68 hypothalamus (ARC)<sup>8-12</sup>. To investigate whether low levels of ghrelin underlie lack of hunger in  
69 hibernating squirrels, we measured total and active ghrelin in blood plasma. There was no  
70 significant difference between IBA and active squirrels, and active ghrelin showed an increasing  
71 trend throughout hibernation, albeit insignificant (Fig. 2a-c). Because such high ghrelin levels are  
72 sufficient to induce feeding in active animals, we hypothesized that hibernating squirrels develop  
73 seasonal ghrelin resistance<sup>4,13</sup>. We tested this by monitoring food consumption in active and IBA  
74 squirrels after peripheral injection of ghrelin. As expected, ghrelin potentiated feeding in active  
75 squirrels to levels observed in mice and rats<sup>14-16</sup>, exceeding those of active squirrels after 48  
76 hours of food deprivation (Fig. 2d, e). In stark contrast, ghrelin failed to potentiate food  
77 consumption when injected during IBAs (Fig. 2d).

78 Immunohistochemical analysis of *c-FOS* expression showed that ghrelin injections activated  
79 a subset of ARC neurons in active, but not IBA, animals (Fig. 2f, g), suggesting that AgRP/NPY  
80 neurons have reduced sensitivity to ghrelin during hibernation. In normal physiological  
81 conditions, ghrelin binding to growth-hormone secretagogue receptors (*Ghsrs*) on AgRP/NPY  
82 neurons triggers release of AgRP from nerve terminals<sup>8,17-21</sup>. In contrast, we observed that AgRP  
83 accumulates in neuronal somas during IBAs (Fig. 2h), implying diminished release. Deep  
84 sequencing of the ARC showed similar levels of *Ghsrs* in active and IBA animals (Fig. 2i). Moreover,  
85 *de novo* cloning of the ARC *Ghsr* revealed that > 95% of transcripts in IBA animals represented  
86 the full-length functional *Ghsr* isoform<sup>20</sup> (Fig. 2j). Thus, the absence of a neuronal and behavioral  
87 response to peripheral ghrelin injection in IBA squirrels cannot be attributed to a lack of  
88 functional ghrelin receptors.

89

## 90 **Hibernating squirrels have reduced leptin signaling**

91         To investigate whether additional mechanisms are involved in the lack of hunger drive in  
92 hibernating squirrels, we asked if ARC neurons are sensitive to the satiety hormone leptin during  
93 IBAs. Plasma levels of leptin were slightly elevated in IBAs compared to active animals (Fig. 3a).  
94 In addition, deep sequencing of the ARC as well as *de novo* cloning revealed active-like levels of  
95 expression of both full-length and truncated transcripts of the long isoform leptin receptor  
96 (*Lepr*)<sup>22</sup> in IBA animals (Fig. 3b-c). However, despite the presence of leptin and its receptor during  
97 hibernation, we observed significantly lower expression of the phosphorylated form of the  
98 transcription factor signal transducer and activator of transcription 3 (pSTAT3) – a marker for  
99 leptin signaling in neurons<sup>23</sup> – in the ARC of IBA compared to active animals (Fig. 3d-e). These  
100 data imply that leptin signaling in ARC neurons is reduced in hibernating squirrels.

101

## 102 **Hibernating animals demonstrate central hypothyroidism**

103         Our findings that ARC neurons resist the orexigenic effects of ghrelin and exhibit reduced  
104 leptin signaling during IBAs suggested that the hypothalamic feeding center temporarily shuts  
105 down during hibernation. However, the mechanism responsible for this effect remained unclear.  
106 The action of the thyroid hormone triiodothyronine (T3) in the central nervous system (CNS) has  
107 been implicated in the control of feeding<sup>24–28</sup>. It has further been shown that the excitability of  
108 ARC AgRP/NPY neurons during fasting or ghrelin administration is increased via uncoupling  
109 protein 2 (UCP2)-dependent mitochondrial proliferation<sup>29,30</sup>. We therefore hypothesized that  
110 anorexia during IBA may be due to central T3 deficiency. In support of this, we found more than  
111 two-fold lower levels of hypothalamic T3 during IBA compared to active animals (active: 0.77 ±  
112 0.1 pg/mg tissue; IBA: 0.32 ± 0.05 pg/mg tissue). Interestingly, we also detected a steady decline  
113 in hypothalamic T3 during the active season, reaching levels comparable to those observed  
114 during IBA by the end of the season (Fig. 4a). However, plasma levels of T3 were equivalent in  
115 both groups of animals and remained constant (Fig. 4b), indicating that thyroid hormone  
116 deficiency during hibernation was restricted to the CNS. We also found significantly higher blood  
117 serum levels of thyroxine (T4) – the precursor to T3 – during IBA (Fig. 4c), further supporting the

118 idea that hibernating squirrels exhibit central, but not peripheral, hypothyroidism. Thyroid  
119 hormones canonically exert their action by binding to nuclear thyroid hormone receptors alpha  
120 (*THRA*) and beta (*THRB*)<sup>31</sup>. Single-cell sequencing of ARC neurons revealed that *THRA* and *THRB*  
121 are expressed in AgRP- and pro-opiomelanocortin (POMC)-containing neurons (Fig. 4d), and that  
122 their expression levels are similar in both physiological states (Fig. 4e), suggesting that  
123 hypothyroidism in IBA animals is not caused by receptor downregulation. Together, these data  
124 indicate that central T3 deficiency may underlie the temporary anorexia associated with  
125 hibernation.

126

### 127 **Central T3 infusion rescues hibernation anorexia**

128         Given the difference between peripheral and central levels of T3, we wondered whether  
129 blood brain barrier (BBB) function might be impaired during hibernation. However, 3 kDa dextran  
130 and biocytin injections confirmed that ARC BBB function is equivalent in active and IBA animals  
131 (Fig. 5a, b and Extended Figure 1). Differential transcriptomics in the ARC subsequently revealed  
132 a significant downregulation of monocarboxylate transporter 8 (MCT8) – the thyroid hormone  
133 transporter – in IBA animals (Fig. 5c). Because MCT8 participates in the translocation of both T4  
134 and T3 from the circulation to brain tissue, and then into glial cells and neurons<sup>32–34</sup>, we  
135 hypothesized that hypothalamic T3 deficiency may be due to diminished transport of T3 and T4  
136 into the ARC. To test this theory, we bypassed this transport step by infusing T3 directly into the  
137 mediobasal hypothalamus during IBA and measured its effect on feeding (Fig. 5a). Remarkably,  
138 even though T3 injection failed to induce feeding up to two hours post-injection (Fig. 5e), it  
139 resulted in robust potentiation of feeding over a 24-hour period (Fig. 5f), consistent with its role  
140 as a transcriptional regulator. Thus, the specific deficiency of T3 in the CNS appears to be the  
141 cause of hibernation anorexia.

142

### 143 **Discussion**

144         Anorexia is a severe disorder that impacts quality of human life and can cause death if  
145 symptoms are severe. In humans, it can be triggered by lack of hunger, for example during cancer  
146 cachexia, or in the psychiatric condition anorexia nervosa, in which subjects self-limit eating

147 despite of hunger. However, anorexia is also part of a normal physiological cycle for ground  
148 squirrels, who do not rely on stored food during hibernation. Because premature emergence  
149 from the safety of the underground burrow to search for food would pose a risk of predation,  
150 anorexia constitutes an important safety mechanism that increases survival. In this study, we  
151 found that squirrels exhibit T3 deficiency in the hypothalamus during IBA, and that restoration of  
152 T3 reverses anorexia, demonstrating that long-term suppression of hunger during hibernation is,  
153 at least partially, due to central hypothyroidism. Thyroid hormone deficiency is specific to the  
154 CNS and does not affect peripheral levels of T3 and T4, obviating the adverse effects of  
155 hypothyroidism on internal organs<sup>35,36</sup> and preserving the involvement of thyroid hormones in  
156 increasing thermogenic capacity prior to squirrels entering hibernation.

157 Hibernating squirrels present a naturalistic model in which central thyroid hormone  
158 function is depressed while essential peripheral thyroid function is preserved. Central thyroid  
159 hormone has been implicated in the seasonal shifts in reproduction and food intake in non-  
160 hibernating animals, including Siberian hamsters, sheep, photoperiodic F344 rats<sup>37-40</sup> and  
161 hibernating arctic ground squirrels<sup>41</sup>. Although the precise mechanism of central hypothyroidism  
162 remains to be determined in our model, the data presented here suggest that reduced levels of  
163 MCT8 may underlie hypothalamic thyroid hormone deficiency during hibernation. Future studies  
164 will provide clues to understand the contribution of neurophysiological pathways, including  
165 hormone transport, to human anorexia.

## 166 **Acknowledgements**

167 We thank Lyle Murphy for technical assistance, and members of the Gracheva and Bagriantsev  
168 laboratories for comments and critique throughout the study. We thank Dr. Rachel Perry for  
169 performing the Leptin ELISA.

170 **Funding.** This work was funded by a Gruber Foundation Fellowship (SMM), The Kavli Foundation  
171 (MPP), National Institutes of Health grants R01NS097547 (SNB), and National Science Foundation  
172 grants 1923127 (SNB) and 1754286 (EOG). RDP was supported by a scholarship from  
173 Coordenação de Aperfeiçoamento de Pessoal de Nível Superior (CAPES), Brazil.

174 **Author contributions.** Conceptualization: SMM, EOG, SNB. Data collection: SMM, RDP, MPP, VF,  
175 MS, LV, AK, HC, TLH. DKM supplied squirrels and provided advice on animal husbandry. Funding  
176 acquisition, project administration and supervision: EOG and SNB. Writing: SMM, RDP, EOG, SNB,  
177 TLH with contribution from DKM, MPP, HC.

178 **Competing Interests.** Authors declare that they have no competing interests.

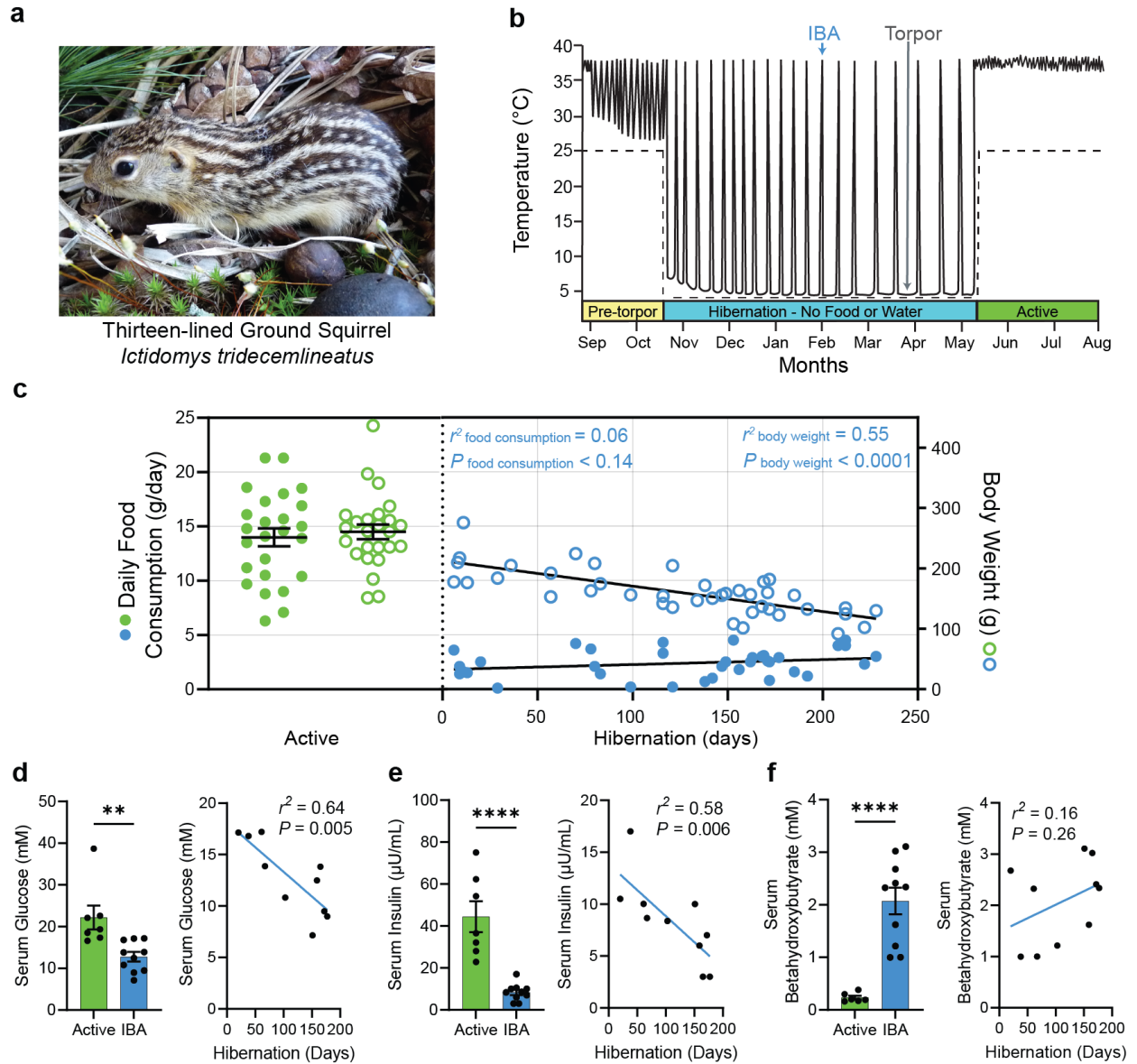
179 **Data and materials availability.** All data are available in the main text or the supplementary  
180 materials. RNA sequencing data are deposited to the Gene Expression Omnibus, accession  
181 number XXXX. Single cell RNA sequencing data are deposited to the to the Gene Expression  
182 Omnibus, accession number XXXX.

183

184

185

186



187

188 **Figure 1: Hibernating ground squirrels have negligible hunger drive.**

189 **a**, Image of a thirteen-lined ground squirrel, *Ictidomys tridecemlineatus*.

190 **b**, Schematic of ground squirrel core body temperature before, during and after hibernation. Dotted line, ambient temperature. Every temperature peak during hibernation represents an IBA.

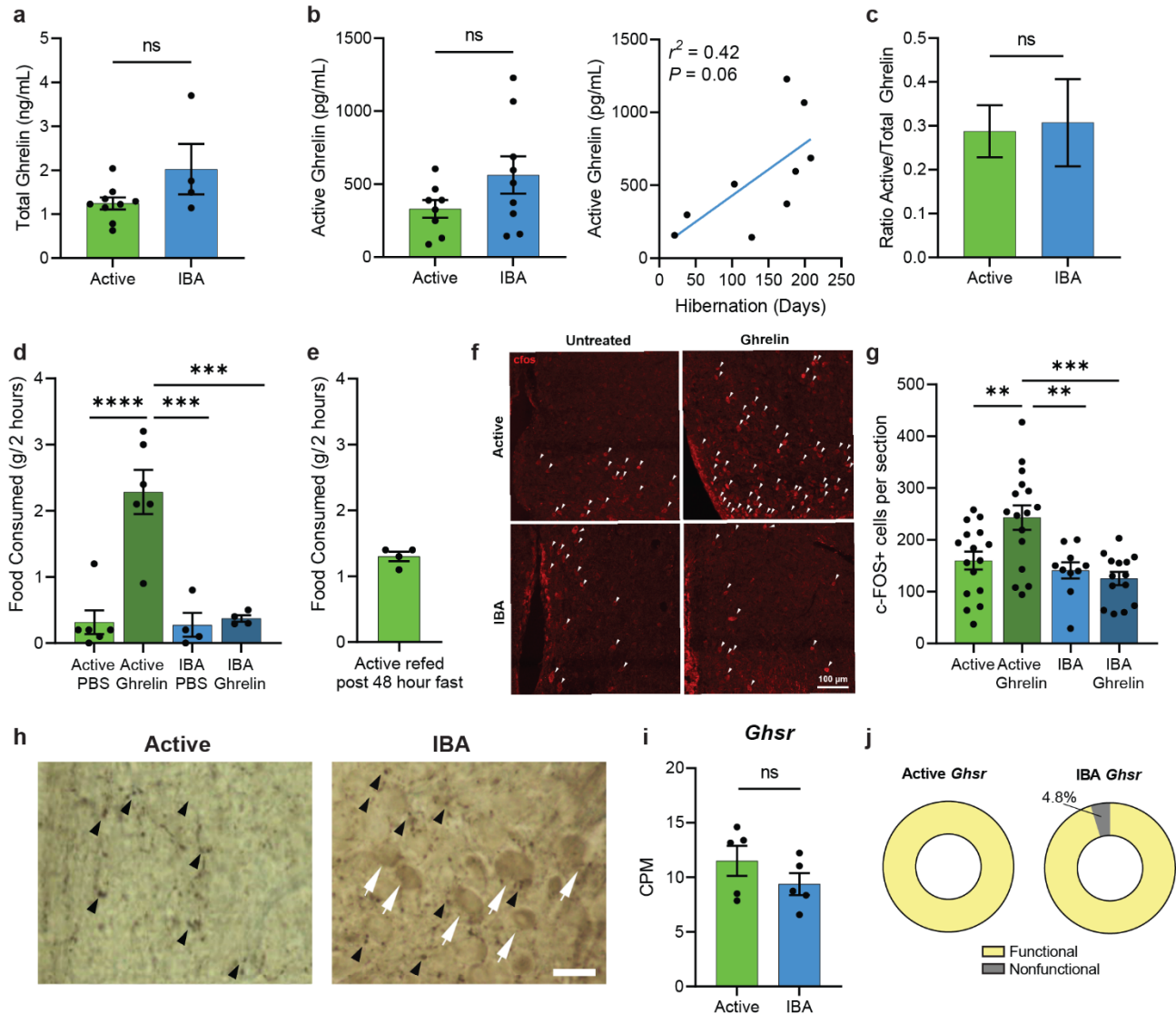
191  
192 **c**, Daily food consumption (left axis, solid points) and body weight (right axis, open circles) during the active (summer) season (green) and hibernation (winter) season (blue). Active feeding data is peak summer food consumption.  $N = 25$  animals. Hibernation feeding and body weight is plotted by days in hibernation.  $N_{IBA(Food)} = 36$ ,  $N_{IBA(Weight)} = 42$  animals.

196 **d to f**, Blood metabolic indicators across active and hibernation states.

197 **d**, Serum glucose,  $N_{Active} = 7$ ,  $N_{IBA} = 10$  animals. **e**, Serum insulin,  $N_{Active} = 7$ ,  $N_{IBA} = 10$  animals. **f**, Serum beta-hydroxybutyrate,  $N_{Active} = 6$ ,  $N_{IBA} = 10$  animals.

199 Data represent mean  $\pm$  SEM in histograms. Each point represents one animal. Student's t-test. Scatter plots are the same data plotted against days in hibernation and fitted with simple linear regressions. **\*\*** $P < 0.01$ , **\*\*\*\*** $P < 0.0001$ .

201



202

203 **Figure 2: Hibernating squirrels demonstrate reversible resistance to ghrelin.**

204 **a**, Plasma level of total and **b**, active (acylated) ghrelin across states (*left*) and throughout hibernation  
 205 (*right*). Total Ghrelin:  $N \geq 4$  animals. Active Ghrelin:  $N \geq 8$  animals. **c**, Ratio of active:total ghrelin. **d**, Two-  
 206 hour food consumption after ghrelin or PBS injection across states.  $N \geq 4$  animals.

207 **e**, Two-hour food consumption in active animals following 48-hour fast.  $N = 4$  animals.

208 **f**, Representative images of ARC c-FOS staining of active and IBA squirrels injected with ghrelin or control.  
 209 Arrowheads, c-FOS+ cells. Scale bar = 100  $\mu\text{m}$ . **g**, Quantification of c-FOS+ cells per section across ARC  
 210 volume.  $N \geq 10$  sections,  $\geq 2$  squirrels.

211 **h**, Representative immuno-EM images of ARC from active and IBA animals. White arrows, neuronal soma;  
 212 black arrowheads, fibers stained for AgRP. Scale bar = 20  $\mu\text{m}$ .

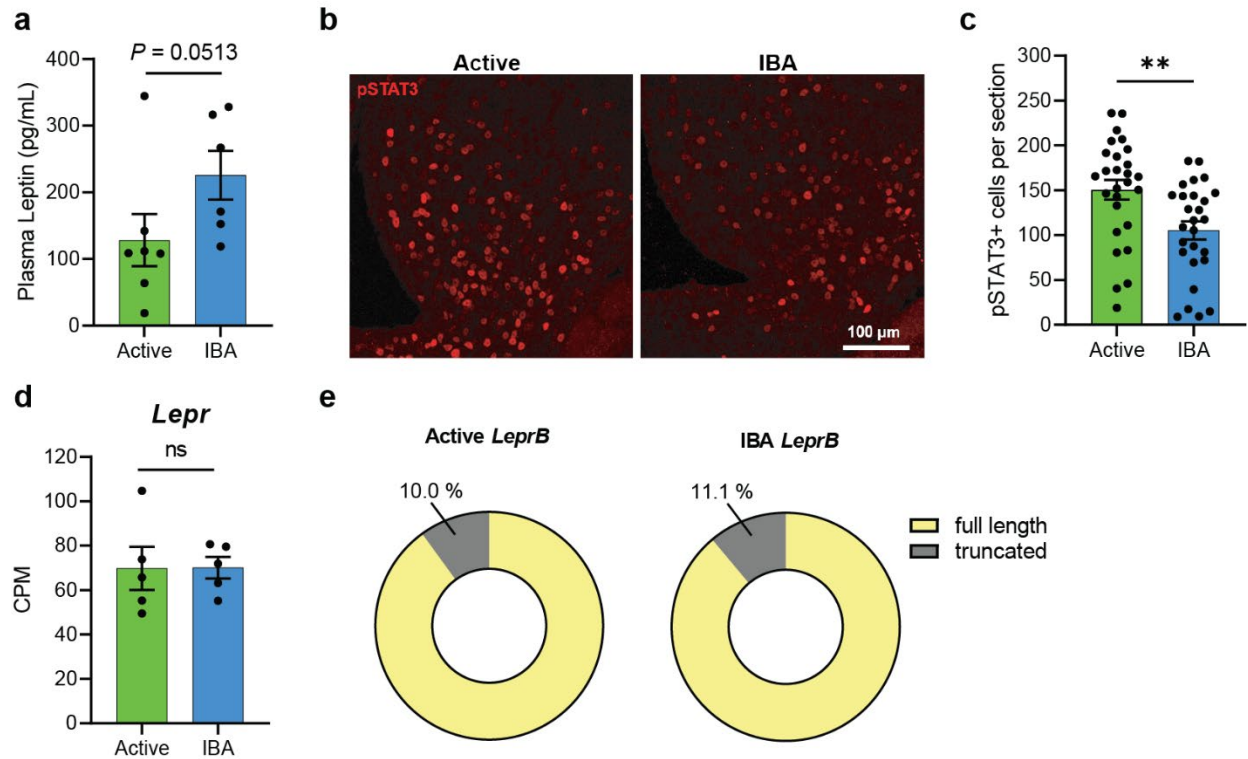
213 **i**, Expression of *Ghser* in the ARC.  $N = 5$  animals.

214 **j**, Quantification of *Ghser* isoforms across states.  $N \geq 38$  clones, 2 squirrels.

215 (**a – i**) Data represented as mean  $\pm$  SEM (**a – c**) Student's t-test.  $**P < 0.01$ ,  $***P < 0.001$ ,  $****P < 0.0001$ .

216 (**d, g**) Two-Way ANOVA followed by Tukey's multiple comparisons.  $**P < 0.01$ ,  $***P < 0.001$ . (**a – e, i**) Each  
 217 point represents one animal. (**g**) Each point represents one section. (**i**)  $FDR > 0.05$ . n.s. = not significant.

218



219

220 **Figure 3: Hibernating squirrels have reduced leptin signaling.**

221 **a**, Plasma leptin levels across states. Data are mean  $\pm$  SEM. Mann-Whitney test,  $N_{Active} = 7$  squirrels,  $N_{IBA} =$

222 6 squirrels.

223 **b**, Expression level of *Lepr* in the ARC. Each point represents one squirrel. Data are mean  $\pm$  SEM,  $FDR >$

224 0.05, ns = not significant.  $N_{Active} = 5$ ,  $N_{IBA} = 5$ .

225 **c**, Quantification of truncated versus full length long-form leptin receptor from full-length de novo cloning

226 in active and IBA squirrels.  $N_{Active} = 10$  clones from 2 squirrels,  $N_{IBA} = 9$  clones from 2 squirrels.

227 **d**, Representative immunohistochemistry images of ARC in active and IBA squirrels using anti-pSTAT3

228 antibody. Scale bar, 100  $\mu\text{m}$ .

229 **e**, Quantification of pSTAT3+ cells per section by state across ARC volume. Each point represents one

230 section. Data are mean  $\pm$  SEM. Student's t-test,  $P < 0.01$ ,  $N_{Active} = 27$  sections from 3 squirrels;  $N_{IBA} = 27$

231 sections from 3 squirrels.

232

233

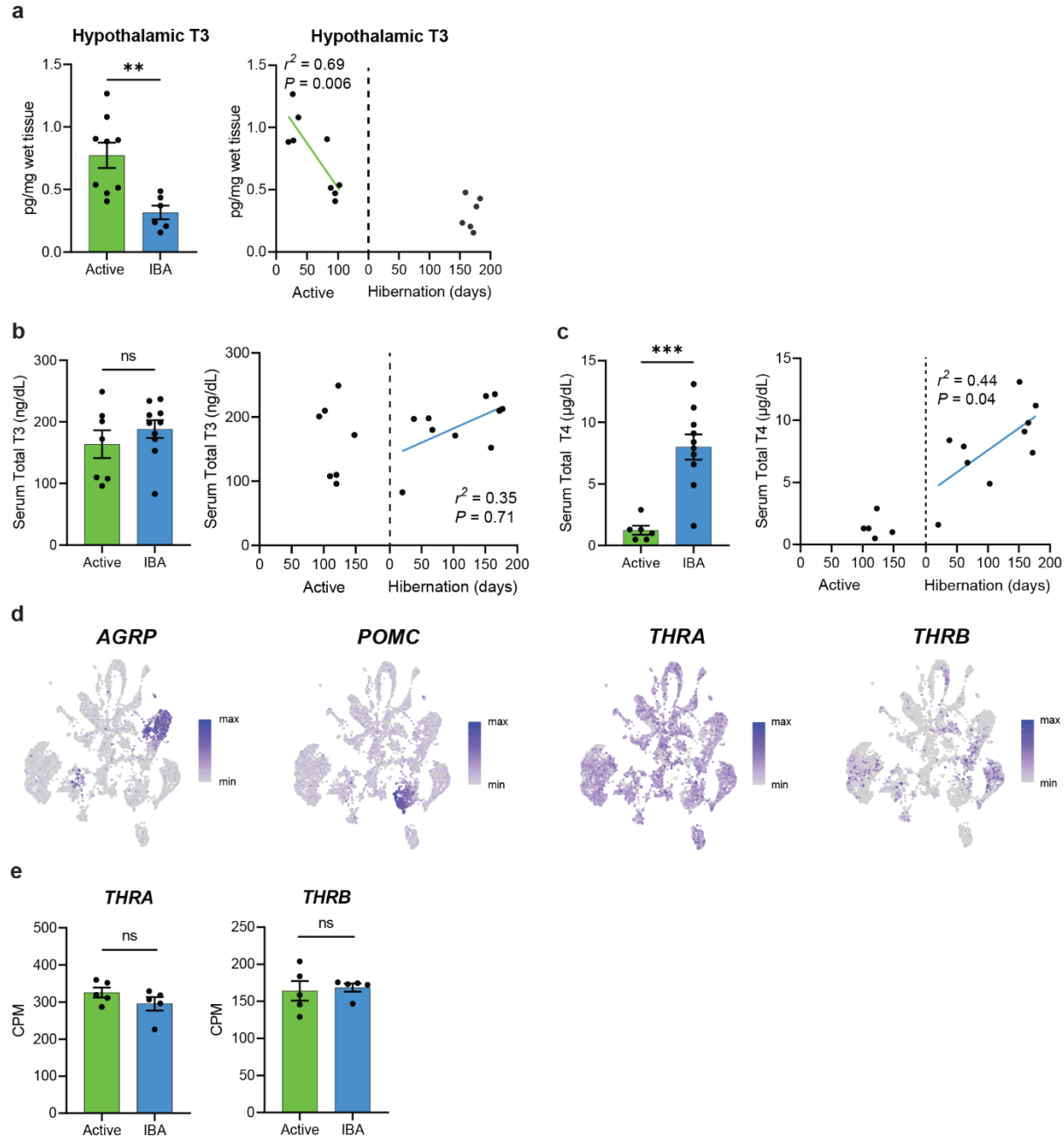
234

235

236

237

238



239

240 **Figure 4: Hibernating animals demonstrate central hypothyroidism.**

241 **a**, T3 content measured from homogenized hypothalamus from active and IBA squirrels.  $N_{Active} = 9$ ,  $N_{IBA} =$   
242 6 animals.

243 **b to c**, Serum total thyroid hormone concentration across active and IBA seasons. **b**, Total T3.  $N_{Active} = 7$ ,  
244  $N_{IBA} = 10$  animals. **c** Total T4.  $N_{Active} = 6$ ,  $N_{IBA} = 10$  animals.

245 **d**, Single cell sequencing shows clusters expressing *Agrp*, *Pomc*, *Thra*, *Thrb*.  $N = 3$  animals.

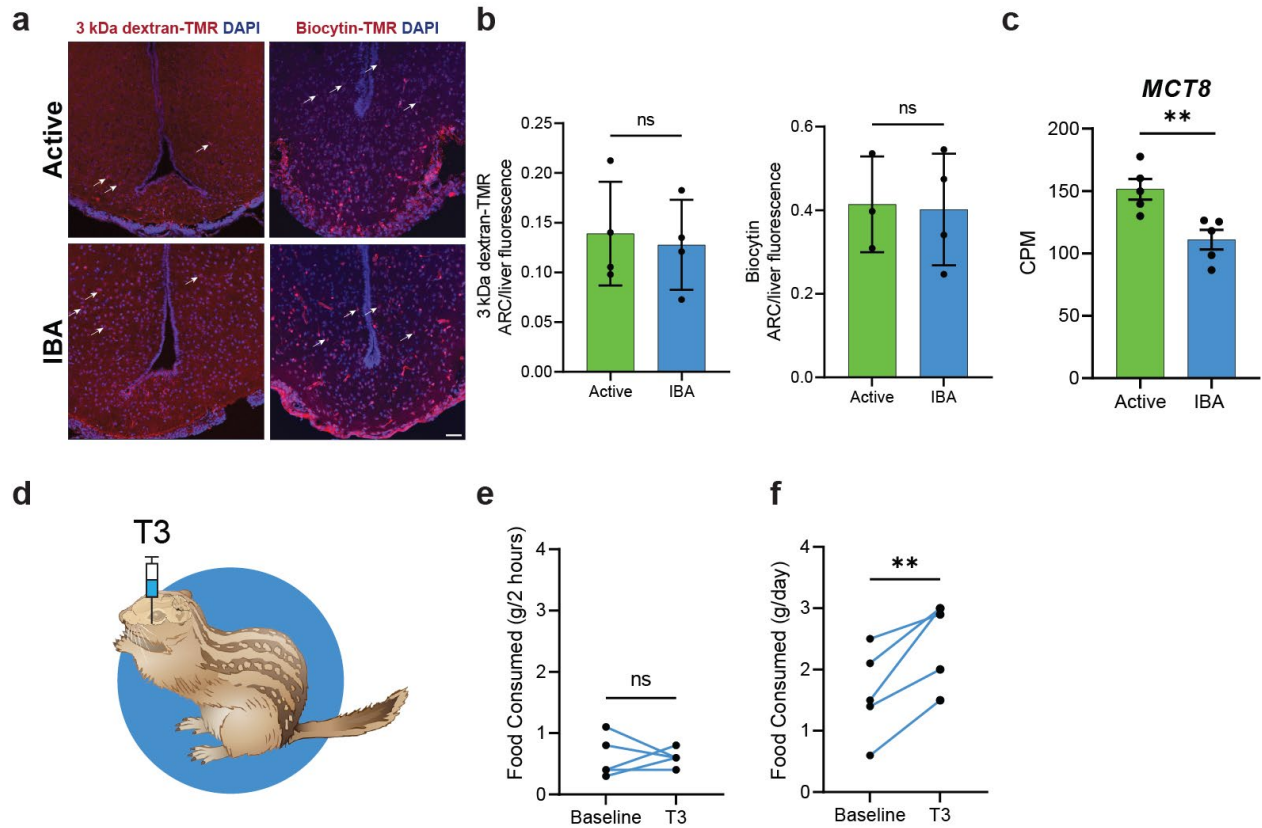
246 **e**, Transcript expression of *Thra* and *Thrb* assessed by RNA sequencing of ARC.  $N_{Active} = 5$ ,  $N_{IBA} = 5$  animals.

247 **(a – c)** Data represent mean  $\pm$  SEM in histograms. Each point represents one animal. Student's t-test. **\*\*** $P$

248  $< 0.01$ , **\*\*\*** $P < 0.001$ , n.s. = not significant. The same data are plotted against days active and days in

249 hibernation and fitted with simple linear regression. **(e)**  $FDR > 0.05$ , n.s. = not significant. Data represent

250 mean  $\pm$  SEM. Each point represents one animal.

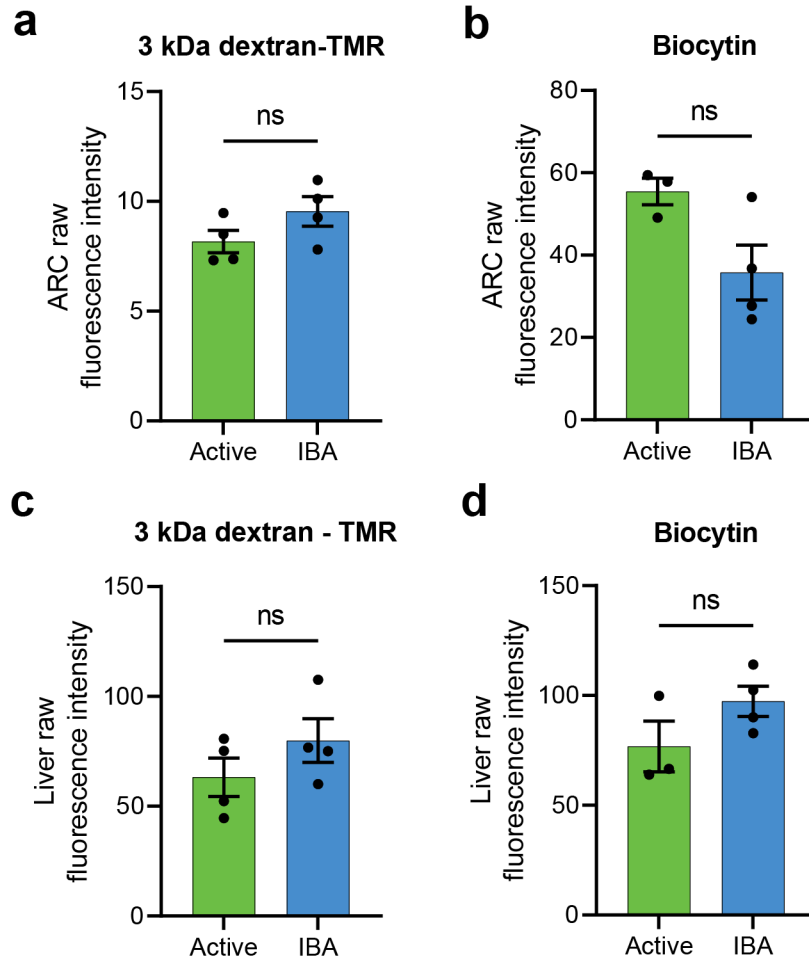


251  
252  
253  
254  
255  
256  
257  
258  
259  
260  
261  
262  
263  
264  
265

**Figure 5: Central T3 infusion rescues hibernation anorexia.**

**a to b**, Blood brain permeability assays by tail artery injection in active and IBA squirrels of 3kDa dextran-tetramethylrhodamine (TMR) and 860 Da biocytin-TMR results in **a**, deposition of dye (white arrows) within the median eminence and ARC. Scale bar = 50  $\mu$ m. **b**, Quantification of normalized fluorescence of 3kDa TMR (left) and 860 Da biocytin-TMR (right). Dextran:  $N_{Active} = 4$ ,  $N_{IBA} = 4$  animals. Biocytin:  $N_{Active} = 3$ ,  $N_{IBA} = 4$  animals. **c**, Level of expression of *MCT8* in the ARC.  $N_{Active} = 5$ ,  $N_{IBA} = 5$  animals. **d to f**, Hypothalamic infusion of T3 during IBA and resulting food consumption. **d**, Schematic of hypothalamic T3 infusion during IBA after arousal from torpor. **e to f**, Paired food consumption at baseline and after T3 infusion at **e**, two-hours and **f** 24-hours.  $N = 5$  animals.

**(b – c)** Data represent mean  $\pm$  SEM. Each point represents one animal. **(b)** Student's t-test. n.s. = not significant. **(c)** **\*\*FDR** < 0.01. **(e – f)** Data are paired with each point representing one animal. Student's Paired t-test. **\*\*P** < 0.01; n.s. = not significant.  $P > 0.05$ .



266  
267  
268  
269  
270  
271  
272  
273  
274  
275  
276  
277  
278  
279  
280  
281  
282  
283  
284  
285  
286  
287

**Extended Figure 1: Raw fluorescence intensity of dyes.**

Quantification of raw fluorescence intensity for 3kDa dextran-TMR and biocytin-TMR in **a to b**, ARC and **c to d**, liver. Data represent mean  $\pm$  SEM with each point representing one animal.  $N \geq 3$  per group. Student's t-test.  $P > 0.05$ . n.s. = not significant.

## 288 References

- 289 1. Aristotle. *The History of Animals*. vol. Book 8, Part 13-17 (The Internet Classics Archive, 350AD).
- 290 2. Mohr, S. M., Bagriantsev, S. N. & Gracheva, E. O. Cellular, Molecular, and Physiological Adaptations
- 291 of Hibernation: The Solution to Environmental Challenges. *Annu. Rev. Cell Dev. Biol.* **36**, 315–338
- 292 (2020).
- 293 3. Andrews, M. T. Molecular interactions underpinning the phenotype of hibernation in mammals. *J.*
- 294 *Exp. Biol.* **222**, jeb160606 (2019).
- 295 4. Healy, J. E., Bateman, J. L., Ostrom, C. E. & Florant, G. L. Peripheral ghrelin stimulates feeding behavior
- 296 and positive energy balance in a sciurid hibernator. *Horm. Behav.* **59**, 512–519 (2011).
- 297 5. Mrosovsky, N. & Boshes, M. Meal patterns and food intakes of ground squirrels during circannual
- 298 cycles. *Appetite* **7**, 163–175 (1986).
- 299 6. Torke, K. G. & Twente, J. W. Behavior of *Spermophilus lateralis* between Periods of Hibernation. *J.*
- 300 *Mammal.* **58**, 385–390 (1977).
- 301 7. Pulawa, L. K. & Florant, G. L. The Effects of Caloric Restriction on the Body Composition and
- 302 Hibernation of the Golden-Mantled Ground Squirrel (*Spermophilus lateralis*). *Physiol. Biochem. Zool.*
- 303 **73**, 538–546 (2000).
- 304 8. Cowley, M. A. *et al.* The Distribution and Mechanism of Action of Ghrelin in the CNS Demonstrates a
- 305 Novel Hypothalamic Circuit Regulating Energy Homeostasis. *Neuron* **37**, 649–661 (2003).
- 306 9. Gropp, E. *et al.* Agouti-related peptide-expressing neurons are mandatory for feeding. *Nat. Neurosci.*
- 307 **8**, 1289–1291 (2005).
- 308 10. Hahn, T. M., Breininger, J. F., Baskin, D. G. & Schwartz, M. W. Coexpression of *Agrp* and *NPY* in fasting-
- 309 activated hypothalamic neurons. *Nat. Neurosci.* **1**, 271–272 (1998).
- 310 11. Kojima, M. *et al.* Ghrelin is a growth-hormone-releasing acylated peptide from stomach. *Nature* **402**,
- 311 656–660 (1999).
- 312 12. Toshinai, K. *et al.* Upregulation of Ghrelin Expression in the Stomach upon Fasting, Insulin-Induced
- 313 Hypoglycemia, and Leptin Administration. *Biochem. Biophys. Res. Commun.* **281**, 1220–1225 (2001).
- 314 13. Bradley, S. P., Pattullo, L. M., Patel, P. N. & Prendergast, B. J. Photoperiodic regulation of the
- 315 orexigenic effects of ghrelin in Siberian hamsters. *Horm. Behav.* **58**, 647–652 (2010).
- 316 14. Nakazato, M. *et al.* A role for ghrelin in the central regulation of feeding. *Nature* **409**, 194–198 (2001).
- 317 15. Wren, A. M. *et al.* The Novel Hypothalamic Peptide Ghrelin Stimulates Food Intake and Growth
- 318 Hormone Secretion. *Endocrinology* **141**, 4325–4328 (2000).
- 319 16. Asakawa, A. *et al.* Ghrelin is an appetite-stimulatory signal from stomach with structural resemblance
- 320 to motilin. *Gastroenterology* **120**, 337–345 (2001).
- 321 17. Sun, Y., Wang, P., Zheng, H. & Smith, R. G. Ghrelin stimulation of growth hormone release and
- 322 appetite is mediated through the growth hormone secretagogue receptor. *Proc. Natl. Acad. Sci.* **101**,
- 323 4679–4684 (2004).
- 324 18. Nogueiras, R. *et al.* *Bsx*, a Novel Hypothalamic Factor Linking Feeding with Locomotor Activity, Is
- 325 Regulated by Energy Availability. *Endocrinology* **149**, 3009–3015 (2008).
- 326 19. Chen, H. Y. *et al.* Orexigenic Action of Peripheral Ghrelin Is Mediated by Neuropeptide Y and Agouti-
- 327 Related Protein. *Endocrinology* **145**, 2607–2612 (2004).
- 328 20. Yanagi, S., Sato, T., Kangawa, K. & Nakazato, M. The Homeostatic Force of Ghrelin. *Cell Metab.* **27**,
- 329 786–804 (2018).
- 330 21. Sakkou, M. *et al.* A Role for Brain-Specific Homeobox Factor *Bsx* in the Control of Hyperphagia and
- 331 Locomotory Behavior. *Cell Metab.* **5**, 450–463 (2007).
- 332 22. Gorska, E. *et al.* Leptin receptors. *Eur. J. Med. Res.* **15**, 50–54 (2010).
- 333 23. Vaisse, C. *et al.* Leptin activation of Stat3 in the hypothalamus of wild-type and *ob/ob* mice but not
- 334 *db/db* mice. *Nat. Genet.* **14**, 95–97 (1996).

- 335 24. Kong, W. M. *et al.* Triiodothyronine Stimulates Food Intake via the Hypothalamic Ventromedial  
336 Nucleus Independent of Changes in Energy Expenditure. *Endocrinology* **145**, 5252–5258 (2004).
- 337 25. Varela, L. *et al.* Hypothalamic mTOR pathway mediates thyroid hormone-induced hyperphagia in  
338 hyperthyroidism. *J. Pathol.* **227**, 209–222 (2012).
- 339 26. Amin, A., Dhillon, W. S. & Murphy, K. G. The Central Effects of Thyroid Hormones on Appetite. *J. Thyroid*  
340 *Res.* **2011**, (2011).
- 341 27. Diano, S., Naftolin, F., Goglia, F. & Horvath, T. L. Fasting-Induced Increase in Type II Iodothyronine  
342 Deiodinase Activity and Messenger Ribonucleic Acid Levels Is Not Reversed by Thyroxine in the Rat  
343 Hypothalamus\*. *Endocrinology* **139**, 2879–2884 (1998).
- 344 28. Diano, S., Naftolin, F., Goglia, F., Csernus, V. & Horvath, T. L. Monosynaptic Pathway Between the  
345 Arcuate Nucleus Expressing Glial Type II Iodothyronine 5'-Deiodinase mRNA and the Median  
346 Eminence-Projective TRH Cells of the Rat Paraventricular Nucleus. *J. Neuroendocrinol.* **10**, 731–742  
347 (1998).
- 348 29. Coppola, A. *et al.* A Central Thermogenic-like Mechanism in Feeding Regulation: An Interplay between  
349 Arcuate Nucleus T3 and UCP2. *Cell Metab.* **5**, 21–33 (2007).
- 350 30. Andrews, Z. B. *et al.* UCP2 mediates ghrelin's action on NPY/AgRP neurons by lowering free radicals.  
351 *Nature* **454**, 846–851 (2008).
- 352 31. Mullur, R., Liu, Y.-Y. & Brent, G. A. Thyroid Hormone Regulation of Metabolism. *Physiol. Rev.* **94**, 355–  
353 382 (2014).
- 354 32. Wirth, E. K. *et al.* Neuronal 3',3,5-Triiodothyronine (T3) Uptake and Behavioral Phenotype of Mice  
355 Deficient in Mct8, the Neuronal T3 Transporter Mutated in Allan–Herndon–Dudley Syndrome. *J.*  
356 *Neurosci.* **29**, 9439–9449 (2009).
- 357 33. Roberts, L. M. *et al.* Expression of the Thyroid Hormone Transporters Monocarboxylate Transporter-  
358 8 (SLC16A2) and Organic Ion Transporter-14 (SLCO1C1) at the Blood-Brain Barrier. *Endocrinology* **149**,  
359 6251–6261 (2008).
- 360 34. Braun, D. *et al.* Developmental and cell type-specific expression of thyroid hormone transporters in  
361 the mouse brain and in primary brain cells. *Glia* **59**, 463–471 (2011).
- 362 35. Ettleson, M. D. & Papaleontiou, M. Evaluating health outcomes in the treatment of hypothyroidism.  
363 *Front. Endocrinol.* **13**, 1026262 (2022).
- 364 36. Fenneman, A. C., Bruinstroop, E., Nieuwdorp, M., van der Spek, A. H. & Boelen, A. A comprehensive  
365 review of thyroid hormone metabolism in the gut and its clinical implications. *Thyroid* (2022)  
366 doi:10.1089/thy.2022.0491.
- 367 37. Barrett, P. *et al.* Hypothalamic Thyroid Hormone Catabolism Acts as a Gatekeeper for the Seasonal  
368 Control of Body Weight and Reproduction. *Endocrinology* **148**, 3608–3617 (2007).
- 369 38. Herwig, A. *et al.* Photoperiod and acute energy deficits interact on components of the thyroid  
370 hormone system in hypothalamic tanycytes of the Siberian hamster. *Am. J. Physiol.-Regul. Integr.*  
371 *Comp. Physiol.* **296**, R1307–R1315 (2009).
- 372 39. Murphy, M. *et al.* Effects of Manipulating Hypothalamic Triiodothyronine Concentrations on Seasonal  
373 Body Weight and Torpor Cycles in Siberian Hamsters. *Endocrinology* **153**, 101–112 (2012).
- 374 40. Dardente, H., Hazlerigg, D. G. & Ebling, F. J. P. Thyroid hormone and seasonal rhythmicity. *Front.*  
375 *Endocrinol.* **5**, 19 (2014).
- 376 41. Chmura, H. E. *et al.* Hypothalamic remodeling of thyroid hormone signaling during hibernation in the  
377 arctic ground squirrel. *Commun. Biol.* **5**, 1–13 (2022).
- 378

379 **Methods:**

380 **Animals**

381 All experimental procedures were performed in compliance with the Institutional Animal Care  
382 and Use Committee of Yale University (protocol 2021-11497). Thirteen-lined ground squirrels (*Ictidomys*  
383 *tridecemlineatus*; age 0.5 – 3 years) of both sexes were single housed in temperature- and humidity-  
384 controlled facilities at Yale University. All squirrels were implanted with an interscapular temperature  
385 transponder (IPTT-300, BMDS).

386 During the active season (May – August), squirrels were kept at 20 °C under a 12 hour:12 hour  
387 light:dark cycle at 40 – 60% humidity and maintained on a diet of dog food (IAMS) supplemented with  
388 sunflower seeds, superworms, and fresh vegetables (celery and carrots) with *ad libitum* access to water.

389 During hibernation (September – April), hypothermic squirrels (body temperature ~20 °C) were  
390 moved to 4 °C at 40 – 60% humidity under constant darkness, without access to food or water. In this  
391 study, “active” squirrels were those with a constant core body temperature (CBT) of 37 °C during the  
392 active season. “IBA” squirrels were those who had undergone at least one bout of hypothermic torpor  
393 during the hibernation season, but had achieved a CBT of > 32 °C for ≥ 60 minutes, or ≥ 20 minutes for the  
394 central thyroid hormone experiments.

395

396 **Food Consumption and Body Mass Measurement**

397 Food consumption and body weight of active adult animals (n = 25) were measured every 2 weeks  
398 during the active period (May-August). Active animals were moved to the behavioral room kept at 20 °C  
399 under a 12 hour :12 hour light:dark cycle and acclimated overnight. In the morning (9 – 11 AM), each was  
400 weighed, transferred to a clean cage, and allowed to habituate for 30 minutes. Food consumption  
401 measurements were performed with dog food only. Pre-weighed food was added to each cage, and  
402 animals were allowed to feed undisturbed. Food remaining 24 hours later was weighed and used to  
403 calculate daily food consumption. A separate bowl of dog food was kept in the behavior room to control  
404 for weight changes due to ambient humidity, but no difference was found so no correction was needed.  
405 The maximum food consumption per animal for the active season was reported.

406 Hibernating animals entered IBA spontaneously, so their food consumption and body weight  
407 measurements occurred between 11 AM – 8 PM. IBA animals were weighed, transferred to a clean cage  
408 in the hibernaculum kept at 4 °C under constant darkness and allowed to habituate for 30 minutes. Food  
409 consumption measurements were performed with dog food only. Pre-weighed food was added to each  
410 cage, and animals were allowed to feed undisturbed. Food remaining 24 hours later was weighed and  
411 used to calculate daily food consumption. IBA measurements occurred just once during the hibernation  
412 season, to ensure that animals remained naïve to food availability during the winter. A separate bowl of  
413 dog food was kept in the behavior room, kept at 4 °C in constant darkness, to control for weight changes  
414 due to ambient humidity, but no difference was found so no correction was needed.

415 **Blood collection**

416 Animals were euthanized by isoflurane overdose. The chest cavity was opened, the right atrium  
417 of the heart pierced, and trunk blood was collected with a 18G needle and syringe.

418 **Serum hormone and metabolite measurements**

419 Whole blood was allowed to coagulate at room temperature for 30 minutes, then centrifuged at  
420 4 °C at 2000 rcf for 15 minutes. Serum was aliquoted and stored at -80 °C for later use. Serum glucose  
421 (Active: n = 7; IBA: n = 10), insulin (Active: n = 7; IBA: n = 10), beta-hydroxybutyrate (Active: n = 6; IBA: n =  
422 10), total T3 (Active: n = 7; IBA: n = 10), and total T4 measurement (Active: n = 6; IBA: n = 10) were  
423 performed by Antech Diagnostics (Fountain Valley, CA).

#### 424 **Plasma ghrelin measurements**

425 Whole blood was collected into chilled, pre-coated K<sub>3</sub>EDTA tubes (MiniCollect, Greiner Bio-One)  
426 and immediately treated with Pefabloc (Sigma) to a final concentration of 1 mM. Blood was centrifuged  
427 at 1600 rcf for 15 minutes. Plasma was aliquoted and stored at -80 °C for later use. Plasma active (acylated)  
428 ghrelin (Active: n = 8; IBA: n = 9) was measured by mouse/rat ELISA (EZRGRA-90K, Millipore). Plasma total  
429 ghrelin (Active: n = 9; IBA: n = 4) was measured by mouse/rat ELISA (EZRGRT-91K, Millipore). All samples  
430 were run in duplicate. The ratio of active (acylated)/ total ghrelin was calculated by dividing the mean of  
431 the active (acylated) ghrelin concentration by the mean of the total ghrelin concentration per state. The  
432 SEM of the ratio was calculated by simple error propagation given by the formula:

$$433 \sigma_{\text{ratio}} = \text{sqrt} ((\sigma A/A)^2 + (\sigma B/B)^2) * A/B$$

434 where A and B are mean values of active (acylated) and total ghrelin, respectively.

#### 435 **Plasma leptin measurements**

436 Whole blood was collected into chilled, pre-coated K<sub>2</sub>EDTA tubes (BD Vacutainer, Lavender/H)  
437 and immediately treated with aprotinin (Millipore Sigma, 9087-70-1) to a final concentration of 0.02 mM.  
438 Blood was centrifuged at 1600 rcf for 15 minutes. Plasma was aliquoted and stored at -80 °C for later use.  
439 Plasma leptin (Active: n = 7, IBA: n = 6) was measured by mouse/rat ELISA (R&D Systems, MOB00). All  
440 samples were run in duplicate. A ROUT outlier test (Q = 1 %) was run to identify one outlier in the Active  
441 state and two outliers in the IBA state.

#### 442 **Intraperitoneal Ghrelin injections**

443 Ground squirrels were acclimated in the behavioral room overnight. Animals were weighed,  
444 transferred to clean cages, and allowed to habituate for 30 minutes. Squirrels were immobilized with  
445 decapicones, injected with 2 mg/kg active (acylated) rat ghrelin (1465, Tocris) solubilized in PBS using an  
446 injection volume of 2 mL/kg body weight, and returned to their cages. Control injections were PBS injected  
447 at a volume of 2 mL/kg body weight. Pre-weighed food was added to the cage and animals allowed to  
448 feed for two hours. The food remaining after the feeding period was weighed and used to calculate food  
449 consumption.

#### 450 **Immunohistochemistry**

451 Ground squirrels were deeply anesthetized by isoflurane inhalation and then subjected to  
452 intracardiac perfusion with PBS followed by fixative [4 % paraformaldehyde in PBS]. Brains were post-  
453 fixed overnight, and transferred to serial 10 %, 20 %, 30 % sucrose solutions after sinking. Brains were  
454 embedded in OCT, frozen on dry ice, and stored at -80 °C until use. Coronal brain sections of the arcuate  
455 nucleus were cut at a thickness of 40 μm on a cryostat (Leica, CM3050S). Sections were mounted onto  
456 SuperFrost Plus slides and stored at -80 °C with desiccant until the day of the immunohistochemistry  
457 procedure. Sections were dried in an incubator at 37 °C for 30 minutes. Slides were washed three times

458 with PBS for 10 minutes, and then washed with 1 % H<sub>2</sub>O<sub>2</sub> and 1 % NaOH in PBS for 10 minutes. Slides  
459 were moved to 0.3 % glycine in PBS 1x for 10 minutes and washed with 0.03 % SDS in PBS. Sections were  
460 blocked for two hours at room temperature with 5 % normal goat serum in 0.5 % PBST.

461 For c-FOS immunohistochemistry after ghrelin injection (Active Untreated: n = 2 animals; Active  
462 ghrelin: n = 2 animals, 16 sections; IBA Untreated: n = 3 animals, 10 sections; IBA Ghrelin: n = 2 animals,  
463 14 sections), sections were incubated with primary antibody (1:500, mouse monoclonal c-FOS C-10, Santa  
464 Cruz, sc-271243) at 4 °C for 48 hours. After incubation with the primary antibody, sections were washed  
465 four times with 0.1 % PBST for 15 minutes. Sections were incubated with secondary antibody (1:500, Alexa  
466 Fluor 647 goat anti-mouse, preadsorbed, Abcam, ab150119) for two hours at room temperature. Sections  
467 were washed four times with 0.1 % PBST for 15 minutes, followed by a wash with PBS.

468 For pSTAT3 immunohistochemistry (Active: n = 3, 27 sections; IBA: n = 3, 27 sections), sections  
469 were incubated with primary antibody (1:200, rabbit polyclonal Phospho-Stat3 (Tyr705), Cell Signaling  
470 Technology, 9131) at 4 °C for 24 hours. After incubation with the primary antibody, sections were washed  
471 five times with 0.1 % PBST for 10 minutes. Sections were incubated with secondary antibody (1:1000,  
472 Alexa Fluor 555 goat anti-rabbit, Abcam, ab150086) for 2 hours at room temperature. Sections were  
473 washed five times with 0.1 % PBST for 15 minutes, followed by a wash with PBS.

474 Slides were mounted using Vectashield with DAPI. Sections were imaged on a Leica SP8 Confocal  
475 Microscope at 20X using the LAS X software. Negative controls (primary antibody omitted) were  
476 performed for c-FOS and pSTAT3 immunohistochemistry and showed no non-specific fluorescent binding.

#### 477 **Immuno-electron microscopy**

478 Ground squirrels were deeply anesthetized by isoflurane inhalation and were subjected to  
479 intracardiac perfusion. Free-floating sections (50 µm thick) were incubated with rabbit anti-AgRP antibody  
480 (Phoenix Pharmaceuticals) diluted 1:2000 in 0.1 M PB after 1 hour blocking in 0.1 M PB with 5% normal  
481 goat serum. After several washes with PB, sections were incubated in the secondary antibody  
482 (biotinylated goat anti-rabbit IgG; 1:250 in PB; Vector Laboratories Inc.) for 2 hours at room temperature,  
483 then rinsed several times in PB followed by incubation for 2 hours at room temperature with avidin-  
484 biotin-peroxidase (ABC; 1:250 in PB; VECTASTAIN Elite ABC kit PK6100, Vector Laboratories). The  
485 immunoreaction was visualized with 3,3-diaminobenzidine (DAB). Sections were then osmicated (1%  
486 osmium tetroxide) for 30 minutes, dehydrated through increasing ethanol concentrations (using 1%  
487 uranyl acetate in 70% ethanol for 30 min), and flat-embedded in Durcupan between liquid release-coated  
488 slides (product no. 70880, Electron Microscopy Sciences). After embedding in Durcupan (14040, Electron  
489 Microscopy Sciences), ultrathin sections were cut on a Leica Ultra-Microtome, collected on Formvar-  
490 coated single-slot grids, and analyzed with a Tecnai 12 Biotwin electron microscope (FEI) with an AMT XR-  
491 16 camera.

#### 492 **Bulk RNA Isolation and Sequencing**

493 Total RNA was isolated from the arcuate nuclei of active (n = 5) and IBA (n = 5) animals that had  
494 been deeply anesthetized by isoflurane inhalation and subjected to intracardiac perfusion with ice cold  
495 PBS. The brain was rapidly dissected and a vibratome (Leica VT1200) was used to cut 300-600 µm coronal  
496 slices posterior to the separation of the optic chiasm. The area surrounding the third ventricle, including  
497 the arcuate nucleus and median eminence, were manually dissected out from the slices using 27G needles

498 and placed immediately into RNA lysis buffer from the Quick-RNA Microprep Kit (Zymo, R1050). Total RNA  
499 was isolated from tissue using the Quick-RNA Microprep Kit (Zymo, R1050). RNA concentration and  
500 integrity number (RIN) were assessed by an Agilent 2100 Bioanalyzer (Agilent, Santa Clara, CA). RNA  
501 concentrations were in the range of ~20 – 400 ng/ $\mu$ L and RIN values were in the range of 7.4 – 9.5.

502 Library preparation and sequencing were carried out at the Yale Center for Genome Analysis.  
503 Sequencing libraries were prepared using the Kapa mRNA Hyper Prep Kit (Cat# KR1352, Roche) including  
504 rRNA depletion. Libraries were sequenced on the Illumina NovaSeq6000 in the 100 bp paired-end mode  
505 according to manufacturer's protocols. A total of ~ 22 – 34 million sequencing read pairs per sample were  
506 obtained.

507 The sequencing data were processed on the Yale Center for Research Computing cluster. Raw  
508 sequencing reads were filtered and trimmed to retain high-quality reads using Trimmomatic v0.39 (1) with  
509 default parameters. Filtered high-quality reads from all samples were aligned to the *Ictidomys*  
510 *tridecemlineatus* reference genome using the STAR aligner v2.7.1a with default parameters (2). The  
511 SpeTri2.0 [GCA\_000236235.1] reference genome and the gene annotation were obtained from the Broad  
512 Institute.

513 The gene annotation was filtered to include only protein-coding genes. Aligned reads were  
514 counted by the featureCounts programs from the Subread package v2.2.0 with default parameters (3).  
515 Read counting was performed at the gene level, i.e. the final read count for each gene included all reads  
516 mapped to all exons of this gene. Differential expression of genes was determined by EdgeR v 3.32.1 (4).  
517 Normalized read counts were obtained by normalizing raw read counts to effective library sizes of each  
518 sample and expressed as reads/million of total reads in a library (CPM). Statistical analysis was performed  
519 using the GLM approach and quasi-likelihood F-test, using a significance value of  $FDR < 0.05$ .

#### 520 **Primary cell dissociation and single-cell RNA Sequencing.**

521 Primary neurons were isolated from the arcuate nucleus of hypothalamus and median eminence  
522 following a published protocol (5) with modification ( $n = 3$ ). Animals were euthanized by isoflurane  
523 inhalation overdose followed by cardiac perfusion with brain perfusion solution (containing in mM: 196  
524 sucrose, 2.5 KCl, 28 NaHCO<sub>3</sub>, 1.25 NaH<sub>2</sub>PO<sub>4</sub>, 7 Glucose, 1 Sodium Ascorbate, 0.5 CaCl<sub>2</sub>, 7 MgCl<sub>2</sub>, 3 Sodium  
525 Pyruvate, oxygenated with 95% O<sub>2</sub>/5% CO<sub>2</sub>, osmolarity adjusted to 300 mOsm with sucrose, pH adjusted  
526 to 7.4). The brain was dissected and slices were cut on a vibratome (Leica, VT1200). A brain slice containing  
527 the ARC and ME were identified by the presence of the third ventricle and separation of the optic chiasm.  
528 Three successive 600- $\mu$ m slices containing the ARC were collected. The area around the third ventricle  
529 was microdissected from the brain slices using a micro-scalpel (Fine Science Tools, 10055-12).

530 Tissue was digested in Hibernate A medium (custom formulation with 2.5 mM glucose and  
531 osmolarity adjusted to 280 mOsm, BrainBits) supplemented with 1 mM lactic acid (Sigma, L1750), 0.5 mM  
532 GlutaMAX (ThermoFisher, 35050061) and 2% B27 minus insulin (ThermoFisher, A1895601) containing 20  
533 U/ml papain (Worthington Biochemical Corporation, LS003124) in a shaking water bath at 34 °C for 30  
534 min and dissociated by mechanical trituration through the tips of glass Pasteur pipettes with decreasing  
535 diameter (0.9 mm, 0.7 mm, 0.5 mm, 0.3 mm). Cell suspension was centrifuged over 8% bovine serum  
536 albumin (Sigma, A9418-5G) layer. Supernatant was removed leaving ~50  $\mu$ l of suspension. Cell suspension  
537 was resuspended in 950  $\mu$ l of Hibernate A medium (same formulation as above) and centrifuged at 300  
538 rcf for 5 min. Supernatant was removed, leaving ~50  $\mu$ l of cell suspension, which was gently mixed with a

539 glass pipette and stored on ice. A 10  $\mu$ l aliquot of cell suspension was mixed with 10  $\mu$ l of Trypan Blue  
540 stain, loaded into a hemocytometer, and used to assess cell concentration and viability.

541 Cell suspension was processed according to the 10X Genomics library preparation protocol at the  
542 Center for Genome Analysis/Keck Biotechnology Resource Laboratory at Yale University. Single cell  
543 suspension in RT Master Mix was loaded on the Single Cell G Chip and partitioned with a pool of about  
544 750,000 barcoded gel beads to form nanoliter-scale Gel Beads-In-Emulsions (GEMs). The volume of cell  
545 suspension for loading was calculated based on cell concentration to capture 10,000 cells. Upon  
546 dissolution of the Gel Beads in a GEM, the primers were released and mixed with cell lysate and Master  
547 Mix. Incubation of the GEMs produced barcoded, full-length cDNA from poly-adenylated mRNA. Silane  
548 magnetic beads were used to remove leftover biochemical reagents and primers from the post GEM  
549 reaction mixture. Full-length, barcoded cDNA was amplified by PCR to generate sufficient mass for library  
550 construction. Enzymatic Fragmentation and Size Selection were used to optimize the cDNA amplicon size  
551 prior to library construction. R1 (read 1 primer sequence) was added to the molecules during GEM  
552 incubation. P5, P7, a sample index, and R2 (read 2 primer sequence) were added during library  
553 construction via End Repair, A-tailing, Adaptor Ligation, and PCR. The final libraries contained the P5 and  
554 P7 primers used in Illumina bridge amplification. Sequencing libraries were sequenced on an Illumina  
555 NovaSeq instrument with 150 bp reads according to the manufacturer's instructions at the depth of ~1.1-  
556 1.4 billion reads/sample.

557  
558 Raw sequencing reads were processed using 10X CellRanger v.6.1.2 (10X Genomics, Pleasanton,  
559 CA). Custom genome reference for thirteen-lined ground squirrel (*Ictidomys tridecemlineatus*) was built  
560 based on the reference genome sequence and annotation obtained from the Ensembl project  
561 ([www.ensembl.org](http://www.ensembl.org) (6) Release 101; all files accessed on 11/20/2020):

562  
563 Genome:  
564 [ftp://ftp.ensembl.org/pub/release-  
565 101/fasta/ictidomys\\_tridecemlineatus/dna/ictidomys\\_tridecemlineatus.SpeTri2.0.dna.toplevel.fa.gz](ftp://ftp.ensembl.org/pub/release-101/fasta/ictidomys_tridecemlineatus/dna/ictidomys_tridecemlineatus.SpeTri2.0.dna.toplevel.fa.gz)

566 Annotation:  
567 [ftp://ftp.ensembl.org/pub/release-  
568 101/gtf/ictidomys\\_tridecemlineatus/ictidomys\\_tridecemlineatus.SpeTri2.0.101.gtf.gz](ftp://ftp.ensembl.org/pub/release-101/gtf/ictidomys_tridecemlineatus/ictidomys_tridecemlineatus.SpeTri2.0.101.gtf.gz)

569  
570 The gene annotation was filtered to include only protein-coding genes using cellranger mkgtf. 10X  
571 CellRanger was used to obtain transcript read counts for each cell barcode, filtered for cell barcodes called  
572 as cells based on the default parameters. Read count matrix was further processed using R 4.2.1, RStudio  
573 2022.02.3, and Seurat 4.1.1 (7). Non-descriptive ground squirrel gene symbols (i.e. those starting with  
574 "ENSSTOG...") were replaced with gene symbols of mouse homolog genes, using the homolog conversion  
575 table from Ensembl. Initial set of cells/barcodes was further filtered to include only those with  $\geq$  500  
576 features/cells,  $\geq$  UMIs/cells, and  $\leq$  10% of mitochondrial genes (defined as those with gene symbol  
577 starting with "MT-"). This resulted in ~11,000-20,000 cells/sample included in the dataset for further  
578 analysis, with the sequencing depth of ~70-100k reads/cell. Read counts were processed according to the  
579 standard Seurat analysis workflow, including normalization, identification of variable features, scaling,  
580 PCA, clustering and visualization using tSNE plots. Graphs report normalized gene expression values.

581  
582 ***De novo* Receptor Cloning**

583 Total RNA from the arcuate nucleus of animals was collected as described above. The remaining  
584 RNA after sequencing was used for *de novo* cloning of *Ghsr* (Active: n = 3; IBA: n = 3) and long-form *Lepr*  
585 (Active: n = 2, 1 female; IBA: n = 2). cDNA was prepared (Invitrogen SuperScript III First-Strand Synthesus  
586 for RT-PCR, 18080-051) and the gene of interest amplified (Phusion High-Fidelity PCR Kit, E0553S) using  
587 the following primers for *Ghsr*: forward 5'- CCAACTTGATCCAGGCTCC -3', reverse 5'-  
588 CAAGTTCGCTGTGCGATGG -3'; and *Lepr*: forward 5'- CAGGTACATGTCTCTGAAGTAAG -3', reverse 5'-  
589 GCCACGTGATCCACTATAATAC -3'. Gel electrophoresis was used to isolate the band of interest and DNA  
590 extracted using the Qiagen Gel Extraction Kit (28704). ORFs were then ligated to topo vector (StrataClone  
591 Blunt PCR Cloning Kit, 240207). cDNA was sent for Sanger Sequencing (Genewiz), and reference sequences  
592 compared the NCBI database.

### 593 **Hypothalamic Infusions**

594 Animals were implanted with abdominal transponders that measured core body temperature,  
595 calibrated between 4 – 40 °C (EMKA Technologies, M1-TA) during the active season, while animals were  
596 euthermic. Animals were allowed to recover for at least 2 weeks before implanted with hypothalamic  
597 infusion cannulas as described below.

598 In a subsequent surgery, infusion cannulas (10 mm 26 G guide, 11 mm 33 G internal, PlasticsOne)  
599 were implanted into the mediobasal hypothalamus during the active season while animals were  
600 euthermic. Briefly, animals were induced into, and maintained at, a stable anesthesia plane using  
601 isoflurane. Animals were administered 0.03 mg/kg preoperative buprenorphine subcutaneously. The  
602 scalp was shaved and the animal transferred to a stereotax, where the skin was sterilized by repeated  
603 applications of betadine and 70% ethanol. Sterile technique was used to expose the skull and drill a hole  
604 to allow for cannula implantation. The following stereotaxic coordinates were utilized for cannula  
605 implantation: 0.5 mm posterior bregma, 0.8 mm lateral midline, 8 mm ventral (guide cannula)/9 mm  
606 ventral (infusion cannula). Two bone screws (2mm long, 1.2 x 0.25 mm thread, McMaster-Carr) and dental  
607 cement (RelyX Unicem Resin, 3M, 56830) were used to anchor the guide cannula to the skull. A dummy  
608 cannula was placed in the guide cannula until experiments were performed. Animals received a dose of  
609 0.4mg/kg meloxicam in 1.5 mL saline subcutaneously immediately after surgery. Animals received post-  
610 operative buprenorphine 0.01 mg/kg and meloxicam 0.2 mg/kg intraperitoneally every 12 hours for 48  
611 hours. Animals were allowed to recover for at least 2 weeks before they were hibernated.

612 Two-hour and daily food consumption were measured in paired IBA animals in two separate  
613 experiments. In the first experiment, feeding was assessed after baseline (no injection) feeding (n = 5) and  
614 triiodothyronine (T3; Sigma, T2877) in the hibernaculum at 4 °C under constant darkness. Control  
615 experiments were performed once IBA patterns appeared stabilized and regular (corresponding to IBA 3  
616 – 4). Animals were allowed to return to torpor after control experiments. Hypothalamic T3 infusion was  
617 performed in the same animals after at least 1 subsequent IBAs had elapsed (corresponding to IBA 5 – 7).

618 In the second experiment, performed in the subsequent year with a new cohort of animals,  
619 hypothalamic infusion of DMSO vehicle (control) (n = 6) (Sigma, D2650) and triiodothyronine (T3; Sigma,  
620 T2877) in the hibernaculum at 4 °C under constant darkness. Control experiments were performed once  
621 IBA patterns appeared stabilized and regular (corresponding to IBA 4 – 12). Animals were allowed to  
622 return to torpor after control experiments. Hypothalamic T3 infusion was performed in the same animals  
623 after at least 2 subsequent IBAs had elapsed (corresponding to IBA 9 – 15).

624 For both experiments, to reduce stress to the animals, infusions were performed while animals  
625 were in the process of arousing from torpor. Animals were identified as IBA candidates when abdominal  
626 temperature exceeded 8 °C. Squirrels were weighed and transferred to a clean cage in the hibernaculum,  
627 kept at 4 °C in constant darkness. When abdominal temperature exceeded 16 °C and interscapular  
628 temperature exceeded 26 °C, a connector assembly consisting of PE50 tubing attached to an infusion  
629 cannula was loaded with control DMSO vehicle or 15.3 mM T3 solubilized in DMSO. At this point, animals  
630 were responsive to touch, but remained curled in the stereotypical torpor position and were unable to  
631 move. An intrahypothalamic dose of either control DMSO or 15.3 nmol T3 was infused in a volume of 1 $\mu$ L  
632 over a time span of three minutes. The infusion cannula was allowed to remain in the guide cannula for  
633 two minutes to allow for the complete diffusion of the infusion solution. The infusion cannula was removed  
634 and replaced with a dummy cannula.

635 During this time, animals continued to warm up. Once the abdominal temperature surpassed 28  
636 °C and the interscapular temperature surpassed 35 °C, animals became mobile and explored their cages.  
637 Animals were allowed to habituate for 20 minutes. The timing of the rewarming process was variable and  
638 took on average around 45 minutes. Dog food was exclusively used for feeding consumption  
639 measurements. After habituation was complete, a pre-weighed amount of food was placed in the cage.  
640 Animals were allowed to feed for 2 hours, at which point the remaining food was removed, weighed, and  
641 returned to the cage. Retrieving and weighing the food took less than 10 minutes per animal. The  
642 remaining food was returned to the cage and the animal allowed to feed for a further 22 hours, to achieve  
643 a 24-hour food consumption measurement.

#### 644 **Hypothalamic Tissue Collection**

645 Naïve animals (Active: n = 9; IBA: n = 6) that had not undergone any experiment were euthanized  
646 by isoflurane overdose and perfused with ice-cold PBS. The brain was removed from the skull and a ~6  
647 mm thick section collected from the optic chiasm to the mamillary bodies using a rat coronal brain matrix  
648 (Electron Microscopy Sciences, 69083-C). The hypothalamus was isolated by removing brain matter above  
649 the top of the third ventricle and lateral to the optic tract. Tissue was flash-frozen in liquid nitrogen and  
650 stored at -80 °C until processing.

#### 651 **Measurement of Hypothalamic T3**

652 Total triiodothyronine (T3) was extracted from frozen hypothalamus tissue (Active: n = 9; IBA: n =  
653 6) and purified as reported previously (8). Briefly, hypothalamic tissue was homogenized in 100%  
654 methanol containing 1 mM 6-propyl-2-thiouracil (PTU) (Sigma, H34203) in a glass-glass tissue grind pestle  
655 (60mm, Kontes, KT885300-0002). Homogenized tissue was centrifuged at 3000 rpm and supernatant  
656 removed. The pellet was resuspended and washed twice more in 100% methanol containing 1 mM PTU.  
657 T3 was extracted from supernatants and purified through solid-phase chromatography using 200 – 400  
658 anion exchange chloride resin (Bio-Rad, 140-1251) in Poly-Prep chromatography columns (Bio-Rad, 731-  
659 1550). Columns were developed with 70% acetic acid (Spectrum, AC110) and washed twice with water.  
660 Supernatants were passed through the column without vacuum. T3 bound to columns was purified  
661 through a series of washes with acetate buffer pH 7.0 and 100% ethanol. T3 was eluted with 2.5 mL 70%  
662 acetic acid. Extracts were evaporated to dryness under nitrogen. T3 concentration was measured by ELISA  
663 (Leinco Technologies, T181). Dried product was resolubilized in the zero-standard and the kit run  
664 according to the manufacturer's instructions.

## 665 **Blood Brain Barrier Tracer Injections and Analysis**

666 Naïve animals (n = 15) that had not undergone any experiment were anesthetized with isoflurane  
667 (4%) in medical air and injected in the tail artery with either biocytin-TMR (ThermoFisher, T12921) or 3kDa  
668 dextran-TMR (ThermoFisher, D3307) at 10 mg/kg. Animals were allowed to recover in their home cage  
669 for 30 minutes until perfusion fixation with 4% paraformaldehyde as described for  
670 Immunohistochemistry.

671 Brains were sectioned on a Leica cryostat at 40  $\mu\text{m}$  and every tenth section was imaged for blood  
672 brain barrier permeability analysis. Sections were rinsed with PBS and coverslipped with Vectashield  
673 containing DAPI (Vector Labs, H-1200). Z-stack images of liver and arcuate nucleus were acquired on a  
674 confocal microscope (Zeiss, LSM-780) using ZEN Software. Maximum intensity projection images were  
675 used for quantification in FIJI.

## 676 **Statistics, analysis, and data collection**

677 Statistical analyses were performed in GraphPad Prism v9.0 or higher (GraphPad Software, San  
678 Diego, CA). Final figures were assembled in Adobe Illustrator. Data were tested for normality using the  
679 Shapiro-Wilk normality test. When normality was assumed, the Student's t-test was used to compare two  
680 groups and Two-Way ANOVA was used to compare multiple groups. Paired data were analyzed with a  
681 paired Student's t-test. Tukey's multiple comparisons test was used to find *post hoc* differences among  
682 groups. When data were not normal, the Mann-Whitney test was used. Sample sizes and statistical data  
683 are reported in the text and figure legends. In the text, values are provided as mean  $\pm$  SEM, and  $P < 0.05$   
684 was considered statistically significant. No blinding was used for data collection. Individuals in  
685 experimental groups were chosen to best match body weight and to represent both sexes across groups.

## 686 **Methods References:**

- 687 1. Bolger, A. M., Lohse, M. & Usadel, B. Trimmomatic: a flexible trimmer for Illumina sequence data.  
688 *Bioinformatics* **30**, 2114–2120 (2014).
- 689 2. Dobin, A. *et al.* STAR: ultrafast universal RNA-seq aligner. *Bioinformatics* **29**, 15–21 (2013).
- 690 3. Liao, Y., Smyth, G. K. & Shi, W. featureCounts: an efficient general purpose program for assigning  
691 sequence reads to genomic features. *Bioinformatics* **30**, 923–930 (2014).
- 692 4. Robinson, M. D., McCarthy, D. J. & Smyth, G. K. edgeR: a Bioconductor package for differential  
693 expression analysis of digital gene expression data. *Bioinformatics* **26**, 139–140 (2010).
- 694 5. Vazirani, R. P., Fioramonti, X. & Routh, V. H. Membrane Potential Dye Imaging of Ventromedial  
695 Hypothalamus Neurons From Adult Mice to Study Glucose Sensing. *J. Vis. Exp. JoVE* 50861 (2013)  
696 doi:10.3791/50861.
- 697 6. Zerbino, D. R. *et al.* Ensembl 2018. *Nucleic Acids Res.* **46**, D754–D761 (2018).
- 698 7. Hao, Y. *et al.* Integrated analysis of multimodal single-cell data. *Cell* **184**, 3573–3587.e29 (2021).
- 699 8. Pinna, G. *et al.* Extraction and quantification of thyroid hormones in selected regions and subcellular  
700 fractions of the rat brain. *Brain Res. Protoc.* **4**, 19–28 (1999).
- 701